Physica Scripta

PAPER

Influence of spontaneously generated coherence on absorption, dispersion, and group index in a five-level cascade atomic system

RECEIVED
17 August 2022

REVISED
13 February 2023

ACCEPTED FOR PUBLICATION
1 March 2023

PUBLISHED
14 March 2023

Le Nguyen Mai Anh[1], **Nguyen Huy Bang**[2], **Nguyen Van Phu**[2,*], **Dinh Xuan Khoa**[2], **Nguyen Thi Ngan**[2], **Bui Thu Huyen**[2] **and Le Van Doai**[2,*]

[1] Faculty of Science, Nong Lam University, Thu Duc City, Ho Chi Minh City, Vietnam
[2] Department of Physics, Vinh University, 182 Le Duan Street, Vinh City, Vietnam
[*] Authors to whom any correspondence should be addressed.

E-mail: phunv@vinhuni.edu.vn **and** doailv@vinhuni.edu.vn

Keywords: spontaneously generated coherence, absorption, dispersion, group index

Abstract

By solving the density matrix equations in the steady state, we have derived analytical expressions for the absorption, dispersion, and group index of a five-level cascade-type atomic system as functions of laser intensity and frequency, spontaneously generated coherence (SGC), and relative phase of applied fields. The influences of SGC and relative phase on absorption, dispersion, and group index of this system under electromagnetically induced transparency (EIT) are studied. It is shown that the three EIT windows of system become deeper and narrower as the strength of SGC increases. These lead to an increase in the slope and the amplitude of the dispersion curves at three EIT windows. As a result, the amplitude of the group index at these three EIT windows also becomes larger when the strength of SGC increases. In particular, the group index can easily be switched between negative and positive values i.e., the light propagation can easily be converted between superluminal to subluminal modes by adjusting the strength of SGC, relative phase or the coupling laser intensity.

1. Introduction

The coherent interaction between an atom with laser fields can produce many quantum interference phenomena in an atomic system which can significantly change the optical properties of the atomic medium. Among them, electromagnetically induced transparency (EIT) [1] has attracted considerable attention due to its interesting applications in quantum and nonlinear optics as well as in modern photonic devices [2]. In addition to suppressed absorption, the dispersion of the medium is also considerably modified in the transparency frequency region, and hence the group index is easily controlled by the parameters of the applied laser fields [3]. Over the past few decades, the EIT and its applications have been widely studied in three-level atomic systems, including lambda-type, V-type, and cascade-type schemes [2]. Recently, studies of EIT have been interested in multi-level atomic systems due to they can generate multiple transparency frequencies [4, 5], which can be applied to modern photonic devices operating at multiple frequencies or multiple channels [2].

In addition to the EIT effect, there is another kind of quantum interference between spontaneous emission channels in the atomic system which can generate an additional atomic coherence, commonly known as spontaneously generated coherence (SGC) [6], and demonstrated experimentally [7]. The SGC can also modify remarkably the optical properties of the atomic medium. The control of absorption and dispersion according to SGC in the three-level atomic systems including lambda-type [8], cascade-type [9] and Vee-type [10] configurations are investigated. It showed that the SGC does not devastate EIT effect, however, the absorption peak on both sides of EIT window becomes larger and the linewidth of absorption profile becomes narrower than the case of the SGC absents. At the same time, the slope of the normal dispersion curve is also steeper in the presence of SGC. This can lead to slower light velocity or subluminal light propagation [11, 12], the transition from optical bistability (OB) to optical multistability (OM) [13], giant Kerr nonlinearity without absorption

[14], enhanced population inversion [15], increasing entanglement in a double quantum dot structure [16], and controlling optical switching and optical soliton [17, 18].

Recent research interest in EIT has been focused on multi-level atomic systems since they can generate multi-EIT windows simultaneously [2]. As demonstrated by McGloin [19], a N-level atomic system excited by N-1 laser fields can obtain N-2 EIT windows. Besides creating the multi-EIT windows, the effect of SGC in multi-level atomic systems have also been realized in several configurations such as four-level N-type system [20, 21], four-level Y-type system [22, 23], double-Λ type four-level system [24] and five-level K-type atomic system [25]. Besides the above numerical studies, there are also some theoretical models of EIT and SGC which are presented in the analytical form [12, 26–29]. Such analytical models show more explicitly the dependence of the atomic optical properties on the laser parameters, therefore the analytical investigations also become easier than those of numerical simulations.

Another simple way to achieve multi-frequency transparency is to use only one pump laser field to couple simultaneously several closely spacing hyperfine levels in atomic system. This way was first experimental demonstrated for ^{85}Rb five-level cascade atomic system by Wang *et al* [30], and obtained three EIT windows on the absorption profile of ^{85}Rb atom. Analytical models of this system have also presented [31, 32] and have shown good agreement with the experimental results [33]. Such analytical models have been applied very successfully for the study of Kerr nonlinearity [34], optical bistability [35], group velocity [36, 37], and optical nano-fibers for guiding entangled beams [38]. However, present works of this five-level cascade EIT system still lack the presence of polarization and phase of laser fields.

In this work, we further develop the analytical model to control the optical properties of the five-level cascade atomic system by the polarization and phase of applied laser fields. By solving the density matrix equations in the steady state, we derive analytical expressions for the absorption, dispersion and group index of the five-level cascade-type atomic system as functions of laser intensity and frequency, spontaneously generated coherence and relative phase. The influences of the SGC and relative phase on absorption, dispersion and group index under electromagnetically induced transparency are considered. Our analytical model may be used for experimental verification of the SGC effect in the five-level cascade atomic system and may be developed to study the dependence of polarization and phase of laser fields on nonlinear optical effects such as Kerr effect, optical bistability, pulse propagation and optical switching, etc.

2. Theoretical model

The five-level cascade-type system interacting two probe and coupling laser fields is illustrated in figure 1. The probe laser E_p with frequency ω_p applies the transition $|1\rangle \leftrightarrow |2\rangle$, while the coupling laser E_c with frequency ω_c couples simultaneously three transitions $|2\rangle \leftrightarrow |3\rangle$, $|2\rangle \leftrightarrow |4\rangle$ and $|2\rangle \leftrightarrow |5\rangle$. The spontaneous decay rate from the state $|2\rangle$ to the ground state $|1\rangle$ is denoted by Γ_1, while Γ_2, Γ_3 and Γ_4 are the spontaneous decay rate from the states $|3\rangle$, $|4\rangle$ and $|5\rangle$ to the state $|2\rangle$, respectively. The frequency detunings of the probe and coupling lasers from the relevant atomic transitions are respectively defined by:

$$\Delta_p = \omega_p - \omega_{21},\ \Delta_c = \omega_c - \omega_{32} \tag{1}$$

The Rabi frequencies of probe and coupling fields are:

$$\Omega_p = \vec{d}_{21} \cdot \vec{E}_p/\hbar \text{ and } \Omega_c = \vec{d}_{32} \cdot \vec{E}_c/\hbar, \tag{2}$$

with d_{ij} is the electric dipole moment between the states $|i\rangle$ and $|j\rangle$.

In the case of the two dipole moments are nonorthogonal, the angle θ between the two dipole moments $\vec{d}_{21}$ and $\vec{d}_{32}$ is determined by:

$$p = \cos\theta = \frac{\vec{d}_{21}.\vec{d}_{32}}{|\vec{d}_{21}||\vec{d}_{32}|}, \tag{3}$$

is called as the quantum interference parameter resulting from the cross-coupling between spontaneous emission paths $|2\rangle \rightarrow |1\rangle$ and $|3\rangle \rightarrow |2\rangle$. Thus, the parameter p represents the strength of the quantum interference by spontaneous emission processes. When the two dipole moments are orthogonal to each other, i.e., $p = 0$, the SGC disappears. When the two dipole moments are parallel to each, $p = 1$, the SGC is maximal. So, the interference parameter p can be adjusted by controlling the alignments of two dipole moments.

The dynamical evolution of the system including spontaneous emission is governed by the Liouville equation:

$$\dot{\rho} = -\frac{i}{\hbar}[H,\ \rho] + \Lambda\rho, \tag{4}$$

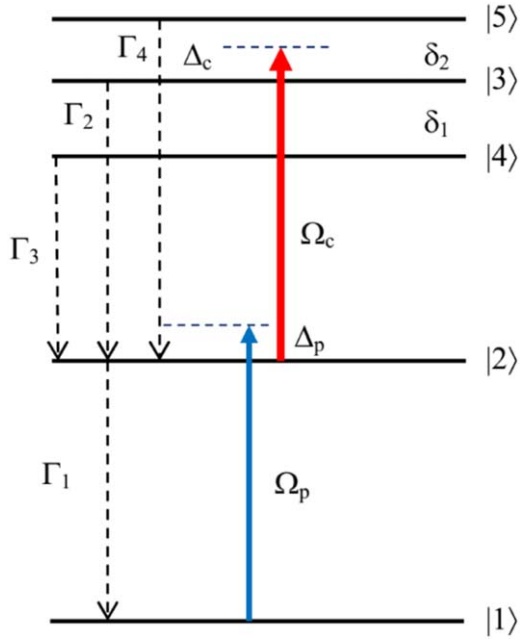

Figure 1. The five-level cascade-type atomic system interacts with probe and coupling laser fields.

where H is the total Hamiltonian which can be written as:

$$H = \sum_{i=1}^{5} \hbar\omega_i |i\rangle\langle i| - \frac{\hbar\Omega_p}{2}(|2\rangle\langle 1|\ e^{-i(\omega_p t+\phi_p)} + c.c)$$

$$-\frac{\hbar\Omega_c}{2}(|3\rangle\langle 2|\ a_{32}e^{-i(\omega_c t+\phi_c)} + |4\rangle\langle 2|\ a_{42}e^{-i(\omega_c t+\phi_c)} + |5\rangle\langle 2|\ a_{52}e^{-i(\omega_c t+\phi_c)} + c.c), \quad (5)$$

with ϕ_p and ϕ_c are the phase of the probe and coupling fields, respectively; $a_{32} = d_{32}/d_{32}$, $a_{42} = d_{42}/d_{32}$, and $a_{52} = d_{52}/d_{32}$ characterize the coupling strengths between the state $|2\rangle$ with three closely-spacing states $|3\rangle$, $|4\rangle$ and $|5\rangle$, respectively.

In the presence of the SGC, the relaxation operator $\Lambda\rho$ of this five-level system is determined by [39]:

$$\begin{aligned}\Lambda\rho = &-\Gamma_1(S_1^+S_1^-\rho + \rho S_1^+S_1^- - 2S_1^-\rho\, S_1^+) - \Gamma_2(S_2^+S_2^-\rho + \rho S_2^+S_2^- - 2S_2^-\rho\, S_2^+)\\ &-\Gamma_3(S_3^+S_3^-\rho + \rho S_3^+S_3^- - 2S_3^-\rho\, S_3^+) - \Gamma_4(S_4^+S_4^-\rho + \rho S_4^+S_4^- - 2S_4^-\rho\, S_4^+)\\ &-\Gamma_{12}(S_1^+S_2^-\rho + \rho S_1^+S_2^- - 2S_2^-\rho\, S_1^+) - \Gamma_{21}(S_2^+S_1^-\rho + \rho S_2^+S_1^- - 2S_1^-\rho\, S_2^+)\\ &-\Gamma_{13}(S_1^+S_3^-\rho + \rho S_1^+S_3^- - 2S_3^-\rho\, S_1^+) - \Gamma_{31}(S_3^+S_1^-\rho + \rho S_3^+S_1^- - 2S_1^-\rho\, S_3^+)\\ &-\Gamma_{14}(S_1^+S_4^-\rho + \rho S_1^+S_4^- - 2S_4^-\rho\, S_1^+) - \Gamma_{41}(S_4^+S_1^-\rho + \rho S_4^+S_1^- - 2S_1^-\rho\, S_4^+)\end{aligned} \quad (6)$$

Here, symmetric and antisymmetric superpositions of the dipole moments as $S_1^- = |1\rangle\langle 2| = \rho_{12}$, $S_1^+ = |2\rangle\langle 1| = \rho_{21}$, $S_2^- = |2\rangle\langle 3| = \rho_{23}$, $S_2^+ = |3\rangle\langle 2| = \rho_{32}$, $S_3^- = |2\rangle\langle 4| = \rho_{24}$, $S_3^+ = |4\rangle\langle 2| = \rho_{42}$, $S_4^- = |2\rangle\langle 5| = \rho_{25}$, $S_4^+ = |5\rangle\langle 2| = \rho_{52}$, with ρ_{ij} is a 5×5 matrix in which the matrix element is in the ith row and the jth column is equal to 1, and the rest is zero; cross-damping rates between the superpositions are defined as $\Gamma_{21} = p\sqrt{\Gamma_1.\Gamma_2}$, $\Gamma_{31} = p\sqrt{\Gamma_1.\Gamma_3}$, $\Gamma_{41} = p\sqrt{\Gamma_1.\Gamma_4}$ and $\Gamma_{ji} = \Gamma_{ij}^*$. After performing matrix calculations, we find the relaxation operator $\Lambda\rho$ as follows:

$$\Lambda\rho = \begin{pmatrix} 2\rho_{22}\Gamma_1 & -\rho_{12}\Gamma_1 + 2\rho_{24}\Gamma_{31} + 2\rho_{23}\Gamma_{21} + 2\rho_{25}\Gamma_{41} & -\rho_{13}\Gamma_2 & -\rho_{14}\Gamma_3 & -\rho_{15}\Gamma_4 \\ -\rho_{21}\Gamma_1 + 2\rho_{42}\Gamma_{13} + 2\rho_{32}\Gamma_{12} + 2\rho_{52}\Gamma_{14} & -2\rho_{22}\Gamma_1 + 2\rho_{33}\Gamma_2 + 2\rho_{44}\Gamma_3 + 2\rho_{55}\Gamma_4 & -\rho_{23}(\Gamma_1+\Gamma_2) & -\rho_{24}(\Gamma_1+\Gamma_3) & -\rho_{25}(\Gamma_1+\Gamma_4) \\ -\rho_{31}\Gamma_2 & -\rho_{32}(\Gamma_1+\Gamma_2) & -2\rho_{33}\Gamma_2 & -\rho_{34}(\Gamma_2+\Gamma_3) & -\rho_{35}(\Gamma_2+\Gamma_4) \\ -\rho_{41}\Gamma_3 & -\rho_{42}(\Gamma_1+\Gamma_3) & -\rho_{43}(\Gamma_3+\Gamma_2) & -2\rho_{44}\Gamma_3 & -\rho_{45}(\Gamma_3+\Gamma_4) \\ -\rho_{51}\Gamma_4 & -\rho_{52}(\Gamma_1+\Gamma_4) & -\rho_{53}(\Gamma_4+\Gamma_2) & -\rho_{54}(\Gamma_4+\Gamma_3) & -2\rho_{55}\Gamma_4 \end{pmatrix}, \quad (7)$$

Using the dipole and rotating wave approximations [39], the density-matrix motion equations can be derived from equations (4)–(7) as:

$$\dot{\rho}_{55} = \frac{i}{2}\Omega_c a_{52}(\rho_{52} - \rho_{25}) - 2\rho_{55}\Gamma_4, \quad (8)$$

$$\dot{\rho}_{44} = \frac{i}{2}\Omega_c a_{42}(\rho_{42} - \rho_{24}) - 2\rho_{44}\Gamma_3, \tag{9}$$

$$\dot{\rho}_{33} = \frac{i}{2}\Omega_c a_{32}(\rho_{32} - \rho_{23}) - 2\rho_{33}\Gamma_2, \tag{10}$$

$$\dot{\rho}_{22} = \frac{i}{2}\Omega_p(\rho_{21} - \rho_{12}) - \frac{i}{2}\Omega_c a_{32}(\rho_{32} - \rho_{23}) - \frac{i}{2}\Omega_c a_{42}(\rho_{42} - \rho_{24}) - \frac{i}{2}\Omega_c a_{52}(\rho_{52} - \rho_{25}) - 2\rho_{22}\Gamma_1 + 2\rho_{33}\Gamma_2 + 2\rho_{44}\Gamma_3 + 2\rho_{55}\Gamma_4, \tag{11}$$

$$\dot{\rho}_{11} = \frac{i}{2}\Omega_p(\rho_{12} - \rho_{21}) + 2\rho_{22}\Gamma_1, \tag{12}$$

$$\dot{\rho}_{54} = [-i(\delta_1 + \delta_2) - (\Gamma_4 + \Gamma_3)]\rho_{54} + \frac{i}{2}\Omega_c a_{42}\rho_{52} - \frac{i}{2}\Omega_c a_{52}\rho_{24}, \tag{13}$$

$$\dot{\rho}_{53} = [-i\delta_2 - (\Gamma_2 + \Gamma_4)]\rho_{53} + \frac{i}{2}\Omega_c a_{32}\rho_{52} - \frac{i}{2}\Omega_c a_{52}\rho_{23}, \tag{14}$$

$$\dot{\rho}_{52} = [i(\Delta_c - \delta_2) - (\Gamma_1 + \Gamma_4)]\rho_{52} + \frac{i}{2}\Omega_p\rho_{51} + \frac{i}{2}\Omega_c a_{32}\rho_{53} + \frac{i}{2}\Omega_c a_{42}\rho_{54} + \frac{i}{2}\Omega_c a_{52}(\rho_{55} - \rho_{22}), \tag{15}$$

$$\dot{\rho}_{51} = [i(\Delta_c + \Delta_p - \delta_2) - \Gamma_4]\rho_{51} + \frac{i}{2}\Omega_p\rho_{52} - \frac{i}{2}\Omega_c a_{52}\rho_{21}, \tag{16}$$

$$\dot{\rho}_{42} = [i(\Delta_c + \delta_1) - (\Gamma_1 + \Gamma_3)]\rho_{42} + \frac{i}{2}\Omega_p\rho_{41} + \frac{i}{2}\Omega_c a_{32}\rho_{43} + \frac{i}{2}\Omega_c a_{52}\rho_{45} + \frac{i}{2}\Omega_c a_{42}(\rho_{44} - \rho_{22}), \tag{17}$$

$$\dot{\rho}_{41} = [i(\Delta_c + \Delta_p + \delta_1) - \Gamma_3]\rho_{41} + \frac{i}{2}\Omega_p\rho_{42} - \frac{i}{2}\Omega_c a_{42}\rho_{21}, \tag{18}$$

$$\dot{\rho}_{43} = [-i\delta_1 - (\Gamma_2 + \Gamma_3)]\rho_{43} - \frac{i}{2}\Omega_c a_{42}\rho_{23} + \frac{i}{2}\Omega_c a_{32}\rho_{42}, \tag{19}$$

$$\dot{\rho}_{32} = [i\Delta_c - (\Gamma_1 + \Gamma_2)]\rho_{32} + \frac{i}{2}\Omega_p\rho_{31} + \frac{i}{2}\Omega_c a_{32}(\rho_{33} - \rho_{22}) + \frac{i}{2}\Omega_c a_{42}\rho_{34} + \frac{i}{2}\Omega_c a_{52}\rho_{35}, \tag{20}$$

$$\dot{\rho}_{31} = [i(\Delta_c + \Delta_p) - \Gamma_2]\rho_{31} + \frac{i}{2}\Omega_p\rho_{32} - \frac{i}{2}\Omega_c a_{32}\rho_{21}, \tag{21}$$

$$\dot{\rho}_{21} = [i\Delta_p - \Gamma_1]\rho_{21} + \frac{i}{2}\Omega_p(\rho_{22} - \rho_{11}) - \frac{i}{2}a_{32}\Omega_c\rho_{31} - \frac{i}{2}\Omega_c a_{42}\rho_{41} - \frac{i}{2}\Omega_c a_{52}\rho_{51} + 2pe^{i\Phi}(\rho_{32}\sqrt{\Gamma_1\Gamma_2} + \rho_{42}\sqrt{\Gamma_1\Gamma_3} + \rho_{52}\sqrt{\Gamma_1\Gamma_4}), \tag{22}$$

where δ_1 and δ_2 are the frequency gaps between the levels $|4\rangle$ - $|3\rangle$ and $|5\rangle$ - $|3\rangle$, respectively. The terms $2pe^{i\Phi}\sqrt{\Gamma_1\Gamma_2}\rho_{32}$, $2pe^{i\Phi}\sqrt{\Gamma_1\Gamma_3}\rho_{42}$ and $2pe^{i\Phi}\sqrt{\Gamma_1\Gamma_4}\rho_{52}$ in equation (22) represent spontaneously generated coherence (SGC), with $\Phi = \phi_p - \phi_c$ is relative phase between probe and coupling fields.

Now, we analytically solve the density matrix equations under the steady-state condition by setting the time derivatives to zero. From equations (8)–(10) and (12), we find the terms ρ_{55}, ρ_{44}, ρ_{33} and ρ_{22}, as follows:

$$\rho_{55} = \frac{\frac{i}{2}\Omega_c a_{52}(\rho_{52} - \rho_{25})}{2\Gamma_4}, \tag{23}$$

$$\rho_{44} = \frac{\frac{i}{2}\Omega_c a_{42}(\rho_{42} - \rho_{24})}{2\Gamma_3}, \tag{24}$$

$$\rho_{33} = \frac{\frac{i}{2}\Omega_c a_{32}(\rho_{32} - \rho_{23})}{2\Gamma_2}, \tag{25}$$

$$\rho_{22} = \frac{\frac{i}{2}\Omega_p(\rho_{21} - \rho_{12})}{2\Gamma_1}, \tag{26}$$

From equations (16), (18) and (21), we derive the terms ρ_{52}, ρ_{42} and ρ_{32} as:

$$\rho_{52} = \frac{\frac{i}{2}\Omega_c a_{52}\rho_{21} - \gamma_{51}\rho_{51}}{\frac{i}{2}\Omega_p}, \tag{27}$$

$$\rho_{42} = \frac{\frac{i}{2}\Omega_c a_{42}\rho_{21} - \gamma_{41}\rho_{41}}{\frac{i}{2}\Omega_p}, \tag{28}$$

$$\rho_{32} = \frac{\frac{i}{2}\Omega_c a_{32}\rho_{21} - \gamma_{31}\rho_{31}}{\frac{i}{2}\Omega_p}, \tag{29}$$

Performing some simple transformations, we obtain:

$$\frac{i}{2}\Omega_c a_{32}(\rho_{32} - \rho_{23}) = \frac{\Omega_c a_{32}}{\Omega_p}\left[\frac{i}{2}\Omega_c a_{32}(\rho_{21} - \rho_{12}) - (\gamma_{31}\rho_{31} + \gamma_{13}\rho_{13})\right], \tag{30}$$

$$\frac{i}{2}\Omega_c a_{42}(\rho_{42} - \rho_{24}) = \frac{\Omega_c a_{42}}{\Omega_p}\left[\frac{i}{2}\Omega_c a_{42}(\rho_{21} - \rho_{12}) - (\gamma_{41}\rho_{41} + \gamma_{14}\rho_{14})\right], \tag{31}$$

$$\frac{i}{2}\Omega_c a_{52}(\rho_{52} - \rho_{25}) = \frac{\Omega_c a_{52}}{\Omega_p}\left[\frac{i}{2}\Omega_c a_{52}(\rho_{21} - \rho_{12}) - (\gamma_{51}\rho_{51} + \gamma_{15}\rho_{15})\right], \tag{32}$$

From equations (23)–(26) and combining with equations (30)–(32), we have:

$$i\Omega_c a_{32}(\rho_{33} - \rho_{22}) = \frac{-\Omega_c^3 a_{32}^3(\rho_{21} - \rho_{12}) - 2i\Omega_c^2 a_{32}^2(\gamma_{31}\rho_{31} + \gamma_{13}\rho_{13})}{4\Gamma_2\Omega_p} + \frac{\Omega_p\Omega_c a_{32}(\rho_{21} - \rho_{12})}{4\Gamma_1}, \tag{33}$$

$$i\Omega_c a_{42}(\rho_{44} - \rho_{22}) = \frac{-\Omega_c^3 a_{42}^3(\rho_{21} - \rho_{12}) - 2i\Omega_c^2 a_{42}^2(\gamma_{41}\rho_{41} + \gamma_{14}\rho_{14})}{4\Gamma_3\Omega_p} + \frac{\Omega_p\Omega_c a_{42}(\rho_{21} - \rho_{12})}{4\Gamma_1}, \tag{34}$$

$$i\Omega_c a_{52}(\rho_{55} - \rho_{22}) = \frac{-\Omega_c^3 a_{52}^3(\rho_{21} - \rho_{12}) - 2i\Omega_c^2 a_{52}^2(\gamma_{51}\rho_{51} + \gamma_{15}\rho_{15})}{4\Gamma_4\Omega_p} + \frac{\Omega_p\Omega_c a_{52}(\rho_{21} - \rho_{12})}{4\Gamma_1}, \tag{35}$$

Substituting equations (33)–(35) into equations (20), (17) and (15), we obtain:

$$(8\Gamma_1\Gamma_2\gamma_{32}\gamma_{31} + 2\Gamma_1\Gamma_2\Omega_p^2 - \Gamma_1\Omega_c^2 a_{32}^2\gamma_{31})\rho_{31} = -\frac{i\Omega_c a_{32}}{2}(\Gamma_1\Omega_c^2 a_{32}^2 - \Gamma_2\Omega_p^2)(\rho_{21} - \rho_{12}) + \Gamma_1\Omega_c^2 a_{32}^2\gamma_{13}\rho_{13} + 4i\Gamma_1\Gamma_2\gamma_{32}\Omega_c a_{32}\rho_{21}, \tag{36}$$

$$(8\Gamma_1\Gamma_3\gamma_{42}\gamma_{41} + 2\Gamma_1\Gamma_3\Omega_p^2 - \Gamma_1\Omega_c^2 a_{42}^2\gamma_{41})\rho_{41} = -\frac{i\Omega_c a_{42}}{2}(\Gamma_1\Omega_c^2 a_{42}^2 - \Gamma_3\Omega_p^2)(\rho_{21} - \rho_{12}) + \Gamma_1\Omega_c^2 a_{42}^2\gamma_{14}\rho_{14} + 4i\Gamma_1\Gamma_3\gamma_{42}\Omega_c a_{42}\rho_{21}, \tag{37}$$

$$(8\Gamma_1\Gamma_4\gamma_{52}\gamma_{51} + 2\Gamma_1\Gamma_4\Omega_p^2 - \Gamma_1\Omega_c^2 a_{52}^2\gamma_{51})\rho_{51} = -\frac{i\Omega_c a_{52}}{2}(\Gamma_1\Omega_c^2 a_{52}^2 - \Gamma_4\Omega_p^2)(\rho_{21} - \rho_{12}) + \Gamma_1\Omega_c^2 a_{52}^2\gamma_{15}\rho_{15} + 4i\Gamma_1\Gamma_4\gamma_{52}\Omega_c a_{52}\rho_{21}, \tag{38}$$

Here,

$\gamma_{21} = i\Delta_p - \Gamma_1$, $\gamma_{31} = i(\Delta_c + \Delta_p) - \Gamma_2$, $\gamma_{41} = i(\Delta_c + \Delta_p + \delta_1) - \Gamma_3$, $\gamma_{51} = i(\Delta_c + \Delta_p - \delta_2) - \Gamma_4$, $\gamma_{32} = i\Delta_c - (\Gamma_1 + \Gamma_2)$, $\gamma_{42} = i(\Delta_c + \delta_1) - (\Gamma_1 + \Gamma_3)$ and $\gamma_{52} = i(\Delta_c - \delta_2) - (\Gamma_1 + \Gamma_4)$. From equations (36)–(38), we get:

$$\rho_{31} = \frac{i(A_1\rho_{12} + A_2\rho_{21})}{A}, \tag{39}$$

$$\rho_{41} = \frac{i(B_1\rho_{12} + B_2\rho_{21})}{B}, \tag{40}$$

$$\rho_{51} = \frac{i(C_1\rho_{12} + C_2\rho_{21})}{C}, \tag{41}$$

where:

$$A = A_{321}A_{321}^* - A_{13}A_{13}^*, \tag{42a}$$

$$A_1 = A_{30}A_{13} - A_{32}^*A_{13} + A_{30}A_{321}^*, \tag{42b}$$

$$A_2 = A_{321}^*A_{32} - A_{30}A_{13} - A_{30}A_{321}^*, \tag{42c}$$

$$A_{321} = 2\Gamma_1(8\Gamma_2\gamma_{32}\gamma_{31} + 2\Gamma_2\Omega_p^2 - \gamma_{31}\Omega_c^2 a_{32}^2), \tag{42d}$$

$$A_{30} = \Omega_c a_{32}(\Gamma_1\Omega_c^2 a_{32}^2 - \Gamma_2\Omega_p^2), \tag{42e}$$

$$A_{13} = 2\Gamma_1\Omega_c^2 a_{32}^2\gamma_{13}, \tag{42f}$$

$$A_{32} = 8\Gamma_1\Gamma_2\gamma_{32}\Omega_c a_{32}. \tag{42g}$$

$$B = B_{421}B_{421}^* - B_{14}B_{14}^*, \tag{43a}$$

$$B_1 = B_{40}B_{14} - B_{42}^*B_{14} - B_{40}B_{421}^*, \tag{43b}$$

$$B_2 = B_{421}^*B_{42} - B_{40}B_{14} - B_{40}B_{421}^*, \tag{43c}$$

$$B_{421} = 2\Gamma_1(8\Gamma_2\gamma_{42}\gamma_{41} + 2\Gamma_2\Omega_p^2 - \gamma_{41}\Omega_c^2 a_{42}^2), \tag{43d}$$

$$B_{40} = \Omega_c a_{42}(\Gamma_1\Omega_c^2 a_{42}^2 - \Gamma_2\Omega_p^2), \tag{43e}$$

$$B_{14} = 2\Gamma_1\Omega_c^2 a_{42}^2\gamma_{14}, \tag{43f}$$

$$B_{42} = 8\Gamma_1\Gamma_2\gamma_{42}\Omega_c a_{42}. \tag{43g}$$

$$C = C_{521}C_{521}^* - C_{15}C_{15}^*, \tag{44a}$$

$$C_1 = C_{50}C_{15} - C_{52}^*C_{15} - C_{50}C_{521}^*, \tag{44b}$$

$$C_2 = C_{521}^*C_{52} - C_{50}C_{15} - C_{50}C_{521}^*, \tag{44c}$$

$$C_{521} = 2\Gamma_1(8\Gamma_2\gamma_{52}\gamma_{51} + 2\Gamma_2\Omega_p^2 - \gamma_{51}\Omega_c^2 a_{52}^2), \tag{44d}$$

$$C_{50} = \Omega_c a_{52}(\Gamma_1\Omega_c^2 a_{52}^2 - \Gamma_2\Omega_p^2), \tag{44e}$$

$$C_{15} = 2\Gamma_1\Omega_c^2 a_{52}^2\gamma_{15}, \tag{44f}$$

$$C_{52} = 8\Gamma_1\Gamma_2\gamma_{52}\Omega_c a_{52}. \tag{44g}$$

with (*) denotes the complex conjugation.

Substituting equations (39)–(41) into equations (27)–(29), we have:

$$\rho_{32} = \frac{\frac{i}{2}\Omega_c a_{32}\rho_{21} - \gamma_{31}\left(\frac{iA_1\rho_{12} + iA_2\rho_{21}}{A}\right)}{\frac{i}{2}\Omega_p}, \tag{45}$$

$$\rho_{42} = \frac{\frac{i}{2}\Omega_c a_{42}\rho_{21} - \gamma_{41}\left(\frac{iB_1\rho_{12} + iB_2\rho_{21}}{B}\right)}{\frac{i}{2}\Omega_p}, \tag{46}$$

$$\rho_{52} = \frac{\frac{i}{2}\Omega_c a_{52}\rho_{21} - \gamma_{51}\left(\frac{iC_1\rho_{12} + iC_2\rho_{21}}{C}\right)}{\frac{i}{2}\Omega_p}, \tag{47}$$

Substituting equations (27)–(29) and equations (45)–(47) into equation (22), and using the initial conditions $\rho_{11}^{(0)} \approx 1$, $\rho_{22}^{(0)} \approx \rho_{33}^{(0)} \approx \rho_{44}^{(0)} \approx \rho_{55}^{(0)} \approx 0$, we find the solution of the density matrix ρ_{21} for the probe response of the medium,

$$\rho_{21} = \frac{-\frac{i}{2}\Omega_p(F_1 + F_2^* + \gamma_{21}^*)}{F_1F_1^* - (\gamma_{21}^* + F_2^*)(\gamma_{21} + F_2)}, \tag{48}$$

Where

$$F_1 = \frac{\Omega_c}{2}\left(\frac{a_{32}A_1}{A} + \frac{a_{42}B_1}{B} + \frac{a_{52}C_1}{C}\right) - \frac{4.e^{i\phi}}{\Omega_p}\left(\frac{A_1}{A}\gamma_{31}\Gamma_{21} + \frac{B_1}{B}\gamma_{41}\Gamma_{31} + \frac{C_1}{C}\gamma_{51}\Gamma_{41}\right), \tag{49}$$

$$F_2 = \frac{\Omega_c}{2}\left(\frac{a_{32}A_2}{A} + \frac{a_{42}B_2}{B} + \frac{a_{52}C_2}{C}\right) - \frac{4.e^{i\phi}}{\Omega_p}\left[\left(\frac{A_2}{A}\gamma_{31}\Gamma_{21} + \frac{B_2}{B}\gamma_{41}\Gamma_{31} + \frac{C_2}{C}\gamma_{51}\Gamma_{41}\right) - \frac{\Omega_c}{2}(a_{32}\Gamma_{21} + a_{42}\Gamma_{31} + a_{52}\Gamma_{41})\right]. \tag{50}$$

The susceptibility of the medium for the probe laser field that is related to ρ_{21} can be written as:

$$\chi = \frac{2Nd_{21}^2}{\varepsilon_0\hbar\Omega_p}\rho_{21} \tag{51}$$

The absorption and dispersion coefficients are given by:

$$\alpha = \frac{\omega_p \mathrm{Im}(\chi)}{c} \tag{52}$$

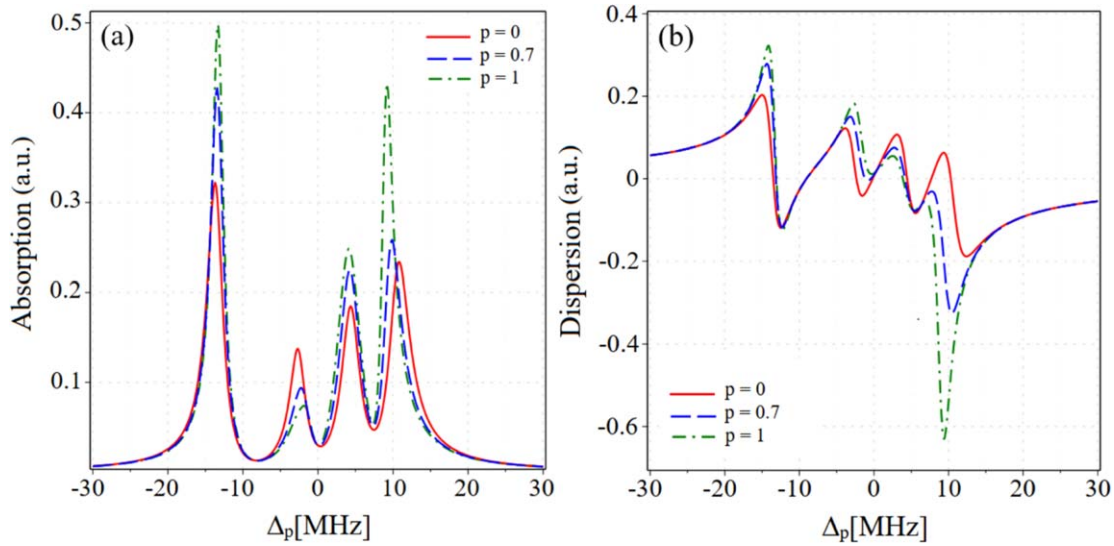

Figure 2. Plots of the absorption (a) and the dispersion (b) versus the probe detuning at the different values of SGC, $p = 0$ (solid line), $p = 0.7$ (dashed line) and $p = 1$ (dash-dotted line). Other parameters are used as $\Omega_c = 10$ MHz, $\Delta_c = 0$ and $\Omega_p = 2$ MHz.

$$n = 1 + \frac{\mathrm{Re}(\chi)}{2} \tag{53}$$

where N is the density of atoms and ε_0 is the permittivity in a vacuum.

The group index n_g which is related to the linear dispersion by the following expression:

$$n_g = n + \omega_p \frac{\partial n}{\partial \omega_p} \tag{54}$$

3. Results and discussion

For the following theoretical investigations, we apply the analytical model to cold ^{85}Rb atom (using MOT, for example) [30] with the states $|1\rangle$, $|2\rangle$, $|3\rangle$, $|4\rangle$ and $|5\rangle$ as $5S_{1/2}(F = 3)$, $5P_{3/2}(F' = 3)$, $5D_{5/2}(F'' = 3)$, $5D_{5/2}(F'' = 4)$ and $5D_{5/2}(F'' = 2)$, respectively. For these states $\delta_1 = 9$ MHz, $\delta_2 = 7.6$ MHz, $\Gamma_1 = 3$ MHz, $\Gamma_2 = \Gamma_3 = \Gamma_4 = 0.5$ MHz, $d_{21} = 1.52 \times 10^{-29}$ C.m, $d_{32} = 1.61 \times 10^{-29}$ C.m, a_{32}:a_{42}:a_{52} = 1:1.46:0.6 and the atomic density $N = 10^8$ atoms/cm^3. The experimental realization of the SGC effect under EIT of this ^{85}Rb atomic system can be found in [40].

In order to investigate the influence of SGC on absorption and dispersion, we fix the parameters of the coupling and probe lasers at $\Omega_c = 10$ MHz, $\Delta_c = 0$ (i.e., the coupling laser is resonant with the transition $|2\rangle \leftrightarrow |3\rangle$) and $\Omega_p = 2$ MHz, and plot the absorption and dispersion coefficients versus the probe detuning for different values of SGC: $p = 0$ (solid line), $p = 0.7$ (dashed line) and $p = 1$ (dash-dotted line) as shown in figure 2. The solid line in figure 2(a) represents the EIT spectrum with three transparency windows at the positions $\Delta_p = 0$, $\Delta_p = -9$ MHz and $\Delta_p = 7.6$ MHz [31]. The solid line in figure 2(b) shows the dispersion spectrum with three normal dispersion curves corresponding to three EIT windows. As the parameter p increases, the absorption profile becomes narrower and the absorption peaks on both sides of each EIT window also become higher. These lead to the slope of the dispersion curves is steeper when the parameter p increases, as we can see in figure 2(b). At the same time, the amplitude of dispersion curves is significantly increased as p increases from 0 to 1.

Thus, absorption and dispersion are controlled according to SGC, so the group velocity of light can also be manipulated versus SGC as shown in figures 3 and 4. In figure 3, we have plotted the group index versus the probe detuning for the different values of SGC, $p = 0$ (solid line), $p = 0.7$ (dashed line), and $p = 1$ (dash-dotted line). Used parameters in figure 3 are similar to those in figure 2. From figure 3 we can see that the large and positive group index (subluminal light) appears at the frequency detunings $\Delta_p = -9$ MHz, $\Delta_p = 0$ and $\Delta_p = 7.6$ MHz corresponding to three EIT windows. Alternating these frequency detunings are those with large and negative group index (superluminal light). The amplitude of the group index also becomes larger when the parameter p increases to 1. In particular, the negative value of the group index is rapidly increased in frequency regions having enhanced dispersion. This means that the group velocity is greatly reduced or accelerated dramatically in the presence of SGC. To see this more clearly, in figure 4(a) we consider the variation of the group

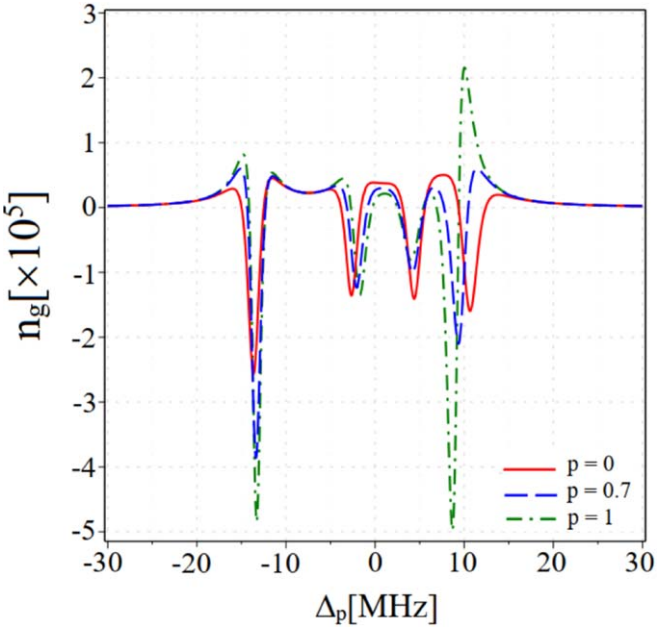

Figure 3. Plots of the group index versus the probe detuning at the different values of $p = 0$ (solid line), $p = 0.7$ (dashed line), and $p = 1$ (dash-dotted line).

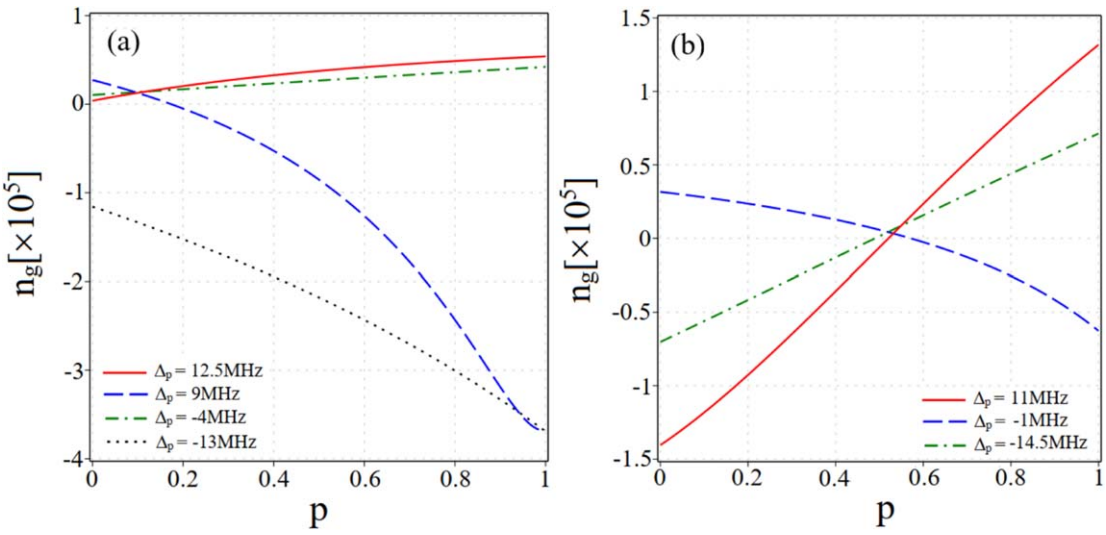

Figure 4. Plots of the group index versus the parameter p at the different values of the probe detuning: variations of amplitude (a) and sign (b) of group index when the parameter p increases from 0 to 1.

index concerning the parameter p at different probe detunings $\Delta_p = -13$ MHz (dotted line) and $\Delta_p = 9$ MHz (dashed line) corresponding to the group index negative peaks, while at $\Delta_p = -4$ MHz (dash-dotted line) and $\Delta_p = 12.5$ MHz (solid line) corresponding to the group index positive peaks in figure 3. Here, other parameters are similar to those in figure 2. It shows that the amplitude of the group index increases (both positive and negative values) as the interference parameter p increases from 0 to 1. Especially, at frequency detunings $\Delta_p = -4$ MHz (dash-dotted line) and $\Delta_p = 12.5$ MHz (solid line), the amplitude of the group index is remarkably enhanced.

In addition, figure 4(b) shows that the interference parameter p can be used as a 'knob' to change the sign of group index between positive to negative values. Here, we have plotted the group index with respect to the parameter p at different probe detunings $\Delta_p = -14.5$ MHz (dash-dotted line), $\Delta_p = -1$ MHz (dashed line) and $\Delta_p = 11$ MHz (solid line) which corresponds to the negative values of group index in figure 3. It is found that the sign of the group index can be varied from negative to positive, or vice versa when adjusting the parameter p

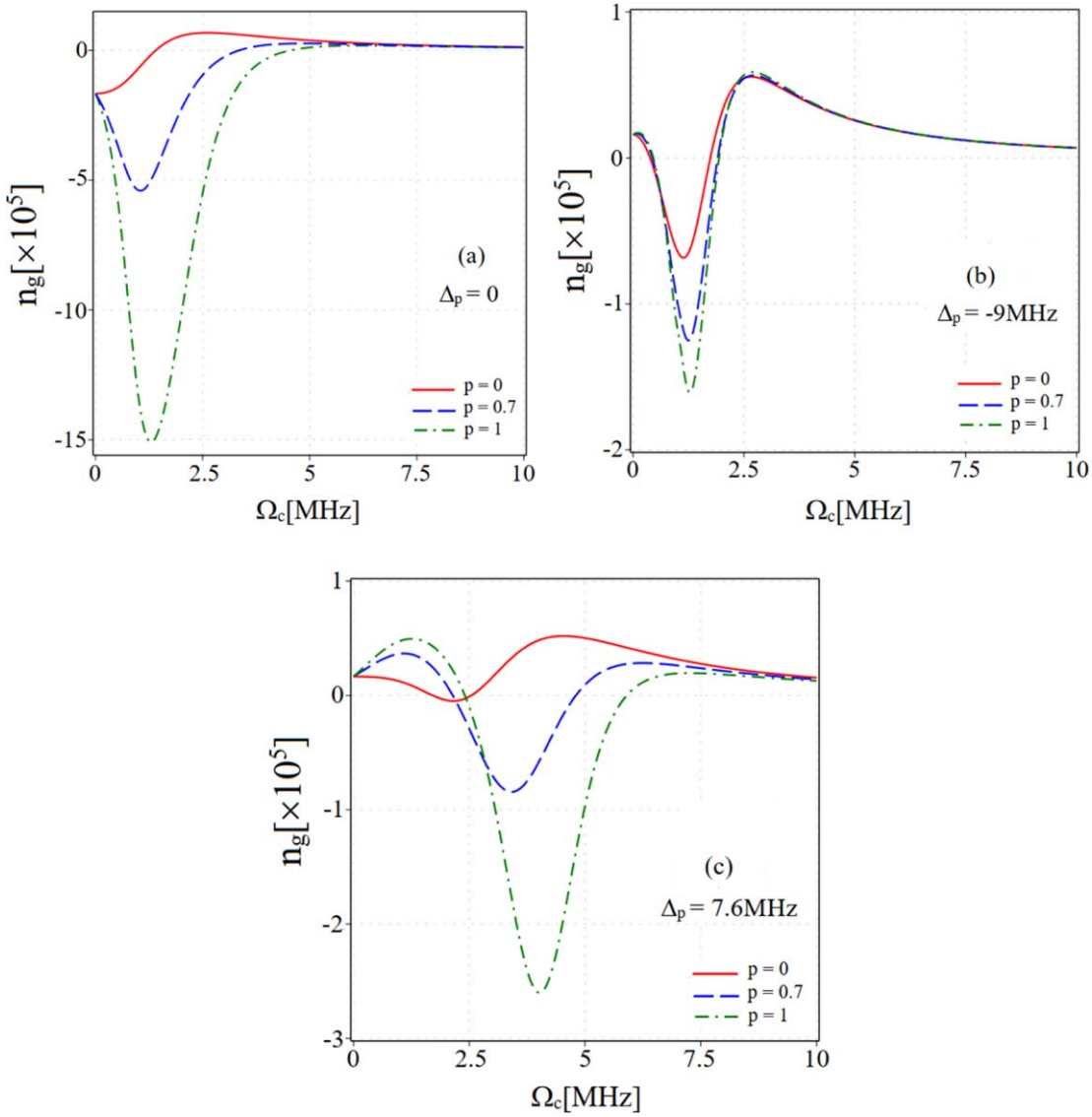

Figure 5. Plots of the group index versus the coupling Rabi frequency at three EIT windows $\Delta_p = 0$ (a), $\Delta_p = -9$ MHz (b) and $\Delta_p = 7.6$ MHz (c), and in the presence of SGC with $p = 0$ (solid line), $p = 0.7$ (dashed line) and $p = 1$ (dash-dotted line). Other parameters are used as $\Delta_c = 0$ and $\Omega_p = 2$ MHz.

from 0 to 1. That is, the light propagation can change from superluminal to subluminal and vice versa by the parameter p.

In figure 5 we consider variations of group index respective to the coupling Rabi frequency at three EIT windows $\Delta_p = 0$ (a), $\Delta_p = -9$ MHz (b) and $\Delta_p = 7.6$ MHz (c) with different values of SGC: $p = 0$ (solid line), $p = 0.7$ (dashed line) and $p = 1$ (dash-dotted line). It shows that at a given probe frequency, the amplitude and sign of the group index are also varied with coupling Rabi frequency, i.e., the group index changes from positive to negative and vice versa when increasing coupling Rabi frequency from 0 to 10 MHz. Specifically, in the resonant frequency region $\Delta_p = 0$ (figure 5(a)) the atomic medium exhibits anomalous dispersion when $\Omega_c = 0$ and hence the group index is negative; gradually increasing the coupling Rabi frequency, the EIT window is formed and the transparency depth increases, so that the medium is changed from anomalous dispersion to normal dispersion and the group index also changes from negative to positive values; then, the group index decreases as the coupling Rabi frequency further increases because the slope of the dispersion curve decreases as the EIT window becomes wider. At the far-resonant frequency regions $\Delta_p = -9$ MHz (figure 5(b)) and $\Delta_p = 7.6$ MHz (figure 5(c)) the medium is normal dispersion when $\Omega_c = 0$ and thus the group index is positive; in the presence of a coupling laser field of small intensity, the EIT has not yet been formed, but the medium is converted to anomalous dispersion and thus the group index is negative; gradually increasing the coupling Rabi frequency, the EIT window is formed and the transparency depth increases, so the medium is also changed from anomalous dispersion to normal dispersion, and the group index also changes from negative to positive. Furthermore, we also find that the group index amplitude in the resonant frequency region is much larger than

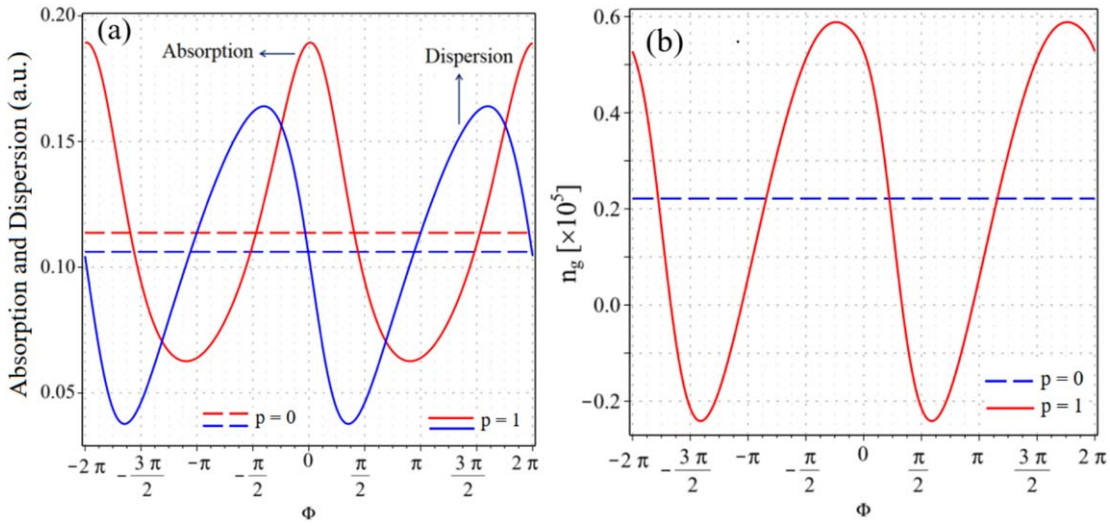

Figure 6. Variations of absorption and dispersion (a), and group index (b) versus relative phase at probe detuning $\Delta_p = 3$ MHz in the presence (solid line) and absence (dash line) of SGC (p = 1 and p = 0) and other parameters of the laser fields as $\Omega_c = 10$ MHz and $\Delta_c = 0$.

that in the far-resonant frequency regions because the slope of the dispersion curve in the resonant region is better than that in the far resonant regions. In addition, in the presence of SGC with $p = 1$, the amplitude of group index is enhanced by several orders of magnitude compared to the case without SGC ($p = 0$). This investigation allows us to choose the optimal parameter of coupling Rabi frequency to achieve the desired group index with positive or negative value.

Finally, we investigate the variations of absorption, dispersion, and group index with respect to the relative phase as depicted in figure 6 in the presence or absence of SGC (p = 1 or p = 0). From the figure we can see that in the absence of SGC (p = 0) the response of the atomic medium does not depend on the relative phase of the laser fields, so the absorption and dispersion coefficients, and group index do not change with relative phase. In contrast, the presence of SGC leads to a phase-sensitive dependence of the optical properties, as we can see in figure 6(a) that at a certain frequency detuning of the probe beam (e.g., in this case $\Delta_p = 3$ MHz), by adjusting the relative phase, the probe beam absorption can be varied from transparent mode to maximum absorption mode and hence the dispersion is also changed from anomalous dispersion (corresponding to maximum absorption) to normal dispersion (corresponding to transparency). As a consequence, the group refractive index also changes in amplitude and sign with relative phase (see figure 6(b)). That is, we can also use the relative phase as a 'knob' to tune the propagation regime of the probe light from superluminal to subluminal and vice versa.

4. Conclusion

The influence of spontaneously generated coherence and relative phase on absorption, dispersion, and group index in a five-level cascade-type atomic system is studied under EIT condition. It showed that the SGC affected all three EIT windows of the system. Specifically, the absorption peaks on both sides of each EIT window are enhanced, while the width of the absorption profile is narrowed when the parameter p increases from 0 to 1. And hence, the slope and the amplitude of the dispersion curves are also significantly increased. As a result, the group index at three EIT windows becomes larger when the SGC strength increases. For this system, in many different frequency ranges the group index can easily be switched between negative and positive values by adjusting the strength of SGC, the relative phase and the coupling laser intensity, i.e., the light propagation can easily be converted between superluminal to subluminal modes. Our analytical model of this five-level system can be useful for experimental observation or related studies such as Kerr nonlinearity, optical bistability, pulse propagation and optical switching with transparent multi-frequency.

Acknowledgments

This research was funded by Nong Lam University Ho Chi Minh City under Grant code CS-CB21-KH-02 and Vietnam Ministry of Education and Training under Grant No. B2022-TDV-05.

Data availability statement

No new data were created or analysed in this study.

ORCID iDs

Nguyen Huy Bang https://orcid.org/0000-0003-4702-3157
Le Van Doai https://orcid.org/0000-0002-1850-3437

References

[1] Boller K J, Imamoglu A and Harris S E 1991 Observation of electromagnetically induced transparency *Phys. Rev. Lett.* **66** 2593
[2] Bang N H, Doai L V and Khoa D X 2019 Controllable optical properties of multiple electromagnetically induced transparency in gaseous atomic media *Comm. Phys.* **28** 1–33
[3] Boyd R W 2009 Slow and fast light: fundamentals and applications *J. Mod. Opt.* **56** 1908–15
[4] Hong Y, Dong Y, Mei Z, Bo F, Yan Z and Hui W J 2012 Absorption and dispersion control in a five-level M-type atomic system *Chin. Phys. B* **21** 114207
[5] Kumar R, Gokhroo V and Chormaic S N 2015 Multi-level cascaded electromagnetically induced transparency in cold atoms using an optical nanofibre interface *New J. Phys.* **17** 123012
[6] Javanainen J 1992 Effect of state superpositions created by spontaneous emission on laser-driven transitions *Europhys. Lett.* **17** 407
[7] Wang C L, Li A J, Zhou X Y, Kang Z H, Yun J and Gao J Y 2008 Investigation of spontaneously generated coherence in dressed states of ^{85}Rb atoms *Opt. Lett.* **33** 687–9
[8] Liu C-p, Gong S-q, Fan X-J and Xu Z-z 2004 Electromagnetically induced absorption via spontaneously generated coherence of a Λ system *Opt. Comm.* **231** 289–95
[9] Ma H M, Gong S Q, Sun Z R, Li R X and Xu Z Z 2006 Effects of spontaneously induced coherence on absorption of a ladder-type atom *Chin. Phys.* **11** 2588
[10] Wang C L, Kang Z H, Tian S C, Jiang Y and Gao J Y 2009 Effect of spontaneously generated coherence on absorption in a V-type system: Investigation in dressed states *Phys. Rev. A* **79** 043810
[11] Ali H, Ahmad I and Ziauddin 2014 Control of group velocity via spontaneous generated coherence and kerr nonlinearity *Comm. Theor. Phys.* **62** 410–6
[12] Bang N H, Anh L N M, Dung N T and Doai L V 2019 Comparative study of light manipulation in three-level systems via spontaneously generated coherence and relative phase of laser fields *Comm. Theo. Phys.* **71** 947–54
[13] Zhu Z, Chen A X, Yang W X and Lee R K 2014 Phase knob for switching steady-state behaviors from bistability to multistability via spontaneously generated coherence *J. Opt. Soc. Am. B* **31** 2061–7
[14] Liang H, Niu Y P, Deng L and Gong S Q 2017 Enhancement of Kerr nonlinearity completely without absorption *Phys. Lett. A* **381** 3978–82
[15] Antón M A, Calderón O G and Carreño F 2005 Spontaneously generated coherence effects in a laser driven four-level atomic system *Phys. Rev. A* **72** 023809
[16] Al-Nashy B, Razzaghi S, Al-Musawi M A, Saghai H R and Al-Khursan A H 2017 Giant gain from spontaneously generated coherence in Y-type double quantum dot structure *Res. Phys.* **7** 2411–6
[17] Dong H M, Bang N H, Khoa D X and Doai L V 2022 All-optical switching via spontaneously generated coherence, relative phase and incoherent pumping in a V-type three-level system *Opt. Commu.* **507** 127731
[18] Dong H M, Doai L V and Bang N H 2018 Pulse propagation in an atomic medium under spontaneously generated coherence, incoherent pumping, and relative laser phase *Opt. Commu.* **426** 553–7
[19] McGloin D, Fullton D J and Dunn M H 2001 Electromagnetically induced transparency in N-level cascade schemes *Opt. Commu.* **190** 221
[20] Wang D and Zheng Y 2011 Quantum interference in a four-level system of a Rb atom: Effects of spontaneously generated coherence *Phys. Rev. A* **83** 013810
[21] Ali H, Khan M, Zubair M, Ahmad P, Khandaker M U, Ali T and Khan F 2020 Control over spectral hole burning via spontaneously generated coherence and Kerr non-linearity *Optik* **224** 165558
[22] Asadpour S H 2013 Optical properties of four level medium via spontaneously generated coherence *Optik* **124** 2305–8
[23] Safari L, Iablonskyi D and Fratini F 2014 Double-electromagnetically induced transparency in a Y-type atomic system *Eur. Phys. J. D* **68** 27
[24] Chen H, Ren J, Gu Y, Zhao D, Zhang J and Gong Q 2016 Nanoscale kerr nonlinearity enhancement using spontaneously generated coherence in plasmonic nanocavity *Sci. Rep.* **5** 18315
[25] Osman K I, Hassan S S and Josh A 2009 Effect of spontaneously generated coherence on EIT and its refractive properties in four- and five-levels systems *Eur. Phys. J. D* **54** 119–30
[26] Menon S and Agarwal G S 1998 Effects of spontaneously generated coherence on the pump-probe response of a Λ system *Phys. Rev. A* **57** 4014
[27] Joshi A, Yang W and Xiao M 2004 Effect of spontaneously generated coherence on the dynamics of multilevel atomic system *Phys. Lett. A* **325** 30–6
[28] Niu Y P and Gong S Q 2006 Enhancing Kerr nonlinearity via spontaneously generated coherence *Phys. Rev. A* **73** 053811
[29] Hazra R and Hossain M M 2021 Effect of spontaneously generated coherence (SGC) on the line shapes of absorption, transparency, dispersion and group index of a four-level inverted Y-type atom-lasers coupling system *Eur. Phys. J. Plus* **136** 761
[30] Wang J, Kong L B, Tu X H, Jiang K J, Li K, Xiong H W, Zhu Y and Zhan M S 2004 Electromagnetically induced transparency in multi-level cascade scheme of cold rubidium atoms *Phys. Lett. A* **328** 437–43
[31] Doai L V, Trong P V, Khoa D X and Bang N H 2014 Electromagnetically induced transparency in five-level cascade scheme of ^{85}Rb atoms: an analytical approach *Optik* **125** 3666–9
[32] Khoa D X, Trong P V, Doai L V and Bang N H 2016 Electromagnetically induced transparency in a five-level cascade system under Doppler broadening: an analytical approach *Phys. Scr.* **91** 035401

[33] Khoa D X, Trung L C, Thuan P V, Doai L V and Bang N H 2017 Measurement of dispersive profile of a multi-window EIT spectrum in a Doppler-broadened atomic medium *J. Opt. Soc. Am. B* **34** 1255–63
[34] Doai L V 2019 Giant cross-Kerr nonlinearity in a six-level inhomogeneously broadened atomic medium *J. Phys. B: At. Mol. Opt. Phys.* **52** 225501
[35] Khoa D X, Doai L V, Anh L N M, Trung L C, Thuan P V, Dung N T and Bang N H 2016 Optical bistability in a five-level cascade EIT medium: an analytical approach *J. Opt. Soc. Am. B* **33** 735–40
[36] Doai L V, An N L T, Khoa D X, Sau V N and Bang N H 2019 Manipulating giant cross-Kerr nonlinearity at multiple frequencies in an atomic gaseous medium *Opt. Soc. Am. B* **36** 2856
[37] Anh L N M, Bang N H, Phu N V, Dong H M, Hien N T T and Doai L V 2023 Slow light amplification in a three-level cascade-type system via spontaneously generated coherence and incoherent pumping *Opt. Quant. Electron.* **55** 246
[38] Kumar R, Gokhroo V and Chormaic S N 2015 Multi-level cascaded electromagnetically induced transparency in cold atoms using an optical nanofibre interface *New J. Phys.* **17** 123012
[39] Patnaik A K and Agarwal G S 1999 Cavity-induced coherence effects in spontaneous emissions from preselection of polarization *Phys. Rev. A* **59** 3015–20
[40] Tian S-C, Kang Z-H, Wang C-L, Wan R-G, Kou J, Zhang H, Jiang Y, Cui H-N and Gao J-Y 2012 Observation of spontaneously generated coherence on absorption in rubidium atomic beam *Opt. Commun.* **285** 294–9